Design, Synthesis and Biological Evaluation of HDAC and VEGFR Dual Inhibitors as a Multi-targeted Anticancer Agents

Xia Xue
The Second Hospital of Shandong University
Yingjie Zhang
Shandong University Cheeloo College of Medicine
Yongxiang Liao
Shandong University Cheeloo College of Medicine
Deqing Sun
The Second Hospital of Shandong University
Lina Li
The Second Hospital of Shandong University
Ying Liu
The Second Hospital of Shandong University
Yongjie Wang
The Second Hospital of Shandong University
Wen Jiang
The Second Hospital of Shandong University
Jian Zhang
The Second Hospital of Shandong University
Yun Luan
The Second Hospital of Shandong University
Xiaogang Zhao (zhaoxiaogang0621@163.com)
The Second Hospital of Shandong University

Research Article

Keywords: Histone deacetylase, vascular endothelial growth factor receptor, polypharmacology, anticancer.multi-target inhibitor

Posted Date: July 26th, 2021

DOI: https://doi.org/10.21203/rs.3.rs-644678/v1

Abstract

Herein a novel series of HDAC and VEGFR dual inhibitors were designed, synthesized and biologically evaluated based on the previously reported pazopanib-based HDAC and VEGFR dual inhibitors. Most target compounds showed significant HDAC1, HDAC6 and VEGFR2 inhibition, which contributed their potent antiproliferative activities against multiple cancer cells lines and significant antiangiogenic potencies in both HUVECs tube formation assay and rat thoracic aorta rings assay. Further HDAC selectivity evaluation indicated that hydroxamic acids **5** and **9e** possessed similar HDAC isoform selectivity profiles to the approved HDAC inhibitor SAHA, while hydrazide **12** presented similar HDAC isoform selectivity profiles to the clinical HDAC inhibitor MS275. The VEGFR inhibition profiles of **5**, **9e** and **12** were similar to that of the approved VEGFR inhibitor pazopanib. The intracellular target engagements of compounds **5** and **12** were confirmed by western blot analysis. Though the mouse liver microsome metabolic stabilities of **5**, **9e** and **12** were inferior to than of pazopanib, these HDAC and VEGFR dual inhibitors provided lead compounds for further structural optimization to get polypharmacological anticancer agents.

Introduction

Targeting epigenetic aberrations is an important strategy for cancer treatment[1].Among the various epigenetic enzymes, histone deacetylases (HDACs) area family of validated anticancer targets with five inhibitors (vorinostat, romidepsin, belinostat, panobinostat and chidamide, **Figure 1**) approved for the treatment of hematologic cancer[2]. Besides epigenetic regulation by removing the acetyl groups from histones, HDACs also play important roles in post-translational modification by deacetylating numerous non-histones [3].

Kinases are one of the most intensively pursued targets in current pharmacological research, especially for cancer, due to their critical roles in regulating protein phosphorylation, one of the most important post-translational modifications involved in signal transductions [4].Vascular endothelial growth factor receptors (VEGFRs) are a family of receptor tyrosine kinases that mediate the biological functions of VEGFs, thereby playing key roles in vascular development. Although many small molecular inhibitors targeting VEGFRs have been approved for the treatment of solid tumors [5], drug resistance and tumor relapse occurred in most patients treated with VEGFRs inhibitors including pazopanib [6-7] (**Figure 1**).

It is worth noting that many preclinical research revealed that combination of HDACs inhibitors and pazopanib held great promise of overcoming pazopanib resistance and enhancing antitumor efficacy [8-10]. More importantly, a recent phase I clinical study showed that targeting epigenetic modification with HDAC inhibitor abexinostat could enhance response and reverse resistance to pazopanib in patients with many solid tumor malignancies[11]. Based on the benefit of HDAC inhibitor and VEGFR inhibitor combination, Zang etc. developed a series of pazopanib-based HDAC and VEGFR dual inhibitors, among which compounds **JMC-13f** and **JMC-6d**(**Figure 2**) exhibited potent HDACs and VEGFRs inhibitory activities, which transformed to their potent antiproliferative activities and antiangiogenic potencies [12].

Inspired by the pioneering work by Zang etc.[12], herein a novel series of pazopanib derivatives were designed and synthesized via structural modification of compounds **JMC-13f** and **JMC-6d**, in the hope of getting novel HDAC and VEGFR dual inhibitors with promising antitumor potency (**Figure 2**).

Materials And Methods

The chemical reagents and solvents were purchased from commercial sources and were used without further purification.^{1}H NMR and ^{13}C NMR spectra were obtained using a Bruker DRX spectrometer at 400 and 100 MHz, respectively. Chemical shifts were reported in parts per million (ppm). Multiplicity of^{1}H NMR signals was reported as singlet (s), doublet (d), triplet (t), quartert (q), and multiplet (m). ESI-MS data were recorded on an API 4000 spectrometer. Melting points were determined using open capillary on an uncorrected electrothermal melting point apparatus.

N-(2-Chloropyrimidin-4-yl)-*N*,2,3-trimethyl-2*H*-indazol-6-amine**(1)**and4-((4-((2,3-dimethyl-2*H*-indazol-6-yl)(methyl)amino)pyrimidin-2-yl)amino)benz-oic acid **(10)** were synthesized as reported methods[12].

4-((4-((2,3-Dimethyl-2*H*-indazol-6-yl)(methyl)amino)pyrimidin-2-yl)amino)phen-ol (**2**).To a solution of **1** (0.50 g,1.74 mmol) and 4-aminophenol (0.23 g, 2.09 mmol) inisopropanol (30 mL) was added 2 drops of conc HCl, and the mixture was heated to reflux with stirring for 4 h. The mixture was cooled to room temperature and the resulting precipitate was collected viafiltration and washed with ethyl acetate, affording compound **2**, white solid(0.43 g, 70%). ESI-MS *m/z*: 360.14 $[M+H]^{+}$.

N^{2}-(4-aminophenyl)-N^{4}-(2,3-dimethyl-2*H*-indazol-6-yl)-N^{4}-methylpyrimidine-2,4-diamine(**3**). To a solution of **1** (0.50 g,1.74 mmol) and benzene-1,4-diamine (0.23 g, 2.09 mmol) inisopropanol (30 mL) was added 2 drops of conc HCl, and the mixture was heated to reflux with stirring for 4 h. The mixture was cooled to room temperature and the resulting precipitate was collected viafiltration and washed with ethyl acetate, affording compound **3**, white solid (0.41 g, 65%). ESI-MS *m/z*: 360.05 $[M+H]^{+}$.

Methyl8-((4-((4-((2,3-dimethyl-2*H*-indazol-6-yl)(methyl)amino)pyrimidin-2-yl)ami-no)phenyl)amino)-8-oxooctanoate(**4**).To a solution of **3** (0.46g, 1.29 mmol) in DMF (10 mL) in ice bath, was added 2-(1H-benzotriazole-1-yl)-1,1,3,3-tetramethyluroniumtetrafluoroborate (TBTU, 0.50 g, 1.54 mmol), followed by Et_3N (0.16 g,1.54 mmol). 30 min later, suberic acid monomethyl ester (0.29 g, 1.54 mmol) was added. 12 h later, the solution was diluted by water and extracted with ethyl acetate. The combined organic extract was washed with saturated $NaHCO_3$and brine, dried over Na_2SO_4overnight, and the solvent was evaporated under vacuum. The crude product was purified by silica gelcolumn chromatography ($MeOH/CH_2Cl_2$, 1/50 to 1/20) to affordcompound**4**, white solid (0.40 g, 58% yield). ESI-MS *m/z*: 530.14 $[M+H]^{+}$.

N^{1}-(4-((4-((2,3-dimethyl-2*H*-indazol-6-yl)(methyl)amino)pyrimidin-2-yl)amino)phe-nyl)-N^{8}-hydroxyoctanediamide (**5**).KOH (28.55g, 509 mmol) and $NH_2OH{\cdot}HCl$ (23.84 g, 343 mmol) were dissolved in 70 mL and 120 mL of MeOH to get solution A and solutionB, respectively. Then solution A was added

dropwise to solution B. After filtering the precipitated KCl, a NH_2OK solution was obtained. Compound **4**(0.25 g, 0.47 mmol) was dissolved in 30 mL of NH_2OK solution and stirred for 2 h. After the reaction was complete, it was evaporated under vacuum. The residue was acidified by addition of 1 M HCl to pH 5-6.The resulting precipitate was collected by filtration and dried to affordcompound**5**, white solid (0.11 g, 43% yield). ^{1}H NMR (400 MHz, DMSO-d_6) δ 10.34 (s, 1H), 9.68 (s, 1H), 9.04 (s, 1H), 8.65 (s, 1H), 7.82 (d, J = 5.9 Hz, 1H), 7.75 (d, J = 8.8 Hz, 1H), 7.61 (d, J = 9.0 Hz, 2H), 7.43 (d, J = 1.7 Hz, 1H), 7.37 (d, J = 8.9 Hz, 2H), 6.88 (dd, J = 8.8, 1.8 Hz, 1H), 5.76 (d, J = 6.0 Hz, 1H), 4.06 (s, 3H), 3.46 (s, 3H), 2.63 (s, 3H), 2.25 (t, J = 7.4 Hz, 2H), 1.94 (t, J = 7.4 Hz, 2H), 1.64 – 1.40 (m, 4H), 1.34 – 1.21 (m, 4H). ^{13}C NMR (101 MHz, DMSO-d_6) δ 171.25, 169.62, 162.89, 158.01, 153.25, 147.39, 142.05, 135.81, 134.08, 132.71, 122.30, 120.07, 119.97, 119.91, 114.48, 96.64, 38.61, 37.86, 36.76, 32.75, 28.89, 25.60, 25.52, 9.89. HRMS (AP-ESI) *m/z* calcd for $C_{28}H_{35}N_8O_3$ $[M+H]^+$531.2832, found 531.2882.

Methyl 6-((4-((4-((2,3-dimethyl-2*H*-indazol-6-yl)(methyl)amino)pyrimidin-2-yl)amin-o)phenyl)amino)hexanoate (**6**).To a solution of **3** (0.40g, 1.11 mmol) in DMF (10 mL), was added potassium carbonate (K_2CO_3, 0.18 g, 1.33 mmol), followed by methyl 6-bromohexanoate (0.28 g,1.33 mmol). The reaction mixture was stirred at 70°C. 12 h later, the solution was diluted by water and extracted with ethyl acetate. The combined organic extract was washed with saturated $NaHCO_3$ and brine, dried over Na_2SO_4 overnight, and the solvent was evaporated under vacuum. The crude product was purified by silica gelcolumn chromatography (MeOH/CH_2Cl_2, 1/50 to 1/20) to afford compound 6, white solid (0.21 g, 39% yield). ESI-MS *m/z*: 488.25 $[M+H]^+$.

Methyl 2-(4-((4-((2,3-dimethyl-2*H*-indazol-6-yl)(methyl)amino)pyrimidin-2-yl)amin-o)phenoxy)acetate (**8a**). To a solution of **2** (0.48g, 1.33 mmol) in DMF (10 mL), was added caesium carbonate (Cs_2CO_3, 0.52 g, 1.60 mmol), followed by methyl bromoacetate (0.24 g,1.60 mmol). The reaction mixture was stirred at 80°C. 6 h later, the solution was diluted by water and extracted with ethyl acetate. The combined organic extract was washed with saturated $NaHCO_3$ and brine, dried over Na_2SO_4 overnight, and the solvent was evaporated under vacuum. The crude product was purified by silica gelcolumn chromatography (MeOH/CH_2Cl_2, 1/50 to 1/20) to affordcompound**8a**, white solid (0.42 g, 73% yield). ESI-MS *m/z*: 433.23 $[M+H]^+$.

Compounds **8b**-**8e** were prepared from compound **2** in a similarmanner as described for compound **8a**, respectively.

Methyl 4-(4-((4-((2,3-dimethyl-2*H*-indazol-6-yl)(methyl)amino)pyrimidin-2-yl)amin-o)phenoxy)butanoate (**8b**). White solid. 70% yield. ESI-MS *m/z*: 461.21 $[M+H]^+$.

Methyl 5-(4-((4-((2,3-dimethyl-2H-indazol-6-yl)(methyl)amino)pyrimidin-2-yl)amin-o)phenoxy)pentanoate (**8c**). White solid. 67% yield. ESI-MS *m/z*: 475.19 $[M+H]^+$.

Methyl 6-(4-((4-((2,3-dimethyl-2*H*-indazol-6-yl)(methyl)amino)pyrimidin-2-yl)amin-o)phenoxy)hexanoate (**8d**). White solid. 65% yield. ESI-MS *m/z*: 489.32 $[M+H]^+$.

Methyl 7-(4-((4-((2,3-dimethyl-2*H*-indazol-6-yl)(methyl)amino)pyrimidin-2-yl)amin-o)phenoxy)heptanoate (**8e**). White solid. 75% yield. ESI-MS *m/z*: 503.31 $[M+H]^+$.

Compounds **7**, **9a**-**9e** were respectively prepared from compound **6**, **8a**-**8e** in a similarmanner as described for compound **5**.

6-((4-((4-((2,3-Dimethyl-2*H*-indazol-6-yl)(methyl)amino)pyrimidin-2yl)amino)pheny-l)amino)-*N*-hydroxyhexanamide (**7**).White solid. 60% yield. ^{1}H NMR (400 MHz, DMSO-d_6) δ 10.33 (s, 1H), 8.80 (s, 1H), 8.64 (s, 1H), 7.74 (t, *J* = 7.7 Hz, 2H), 7.43 (s, 1H), 7.36 (d, *J* = 8.7 Hz, 2H), 6.90 – 6.83 (m, 1H), 6.45 (d, *J* = 8.6 Hz, 2H), 5.69 (d, *J* = 6.1 Hz, 1H), 4.06 (s, 3H), 3.44 (s, 3H), 2.94 (t, *J* = 6.8 Hz, 2H), 2.62 (s, 3H), 1.96 (t, *J* = 7.4 Hz, 2H), 1.53 (p, *J* = 7.2 Hz, 4H), 1.39 – 1.28 (m, 2H). HRMS (AP-ESI) *m/z* calcd for $C_{26}H_{33}N_8O_2$ $[M+H]^+$ 489.2726, found 489.2749.

2-(4-((4-((2,3-Dimethyl-2*H*-indazol-6-yl)(methyl)amino)pyrimidin-2-yl)amino)pheno-xy)-*N*-hydroxyacetamide (**9a**). white solid (0.16 g, 50% yield). 1H NMR (400 MHz, DMSO-d_6) δ 10.78 (s, 1H), 9.07 (s, 1H), 8.93 (s, 1H), 7.80 (d, *J* = 6.1 Hz, 1H), 7.76 (d, *J* = 8.7 Hz, 1H), 7.61 (d, *J* = 8.9 Hz, 2H), 7.44 (s, 1H), 6.88 (dd, *J* = 8.8, 1.5 Hz, 1H), 6.81 (d, *J* = 8.9 Hz, 2H), 5.76 (d, *J* = 6.0 Hz, 1H), 4.39 (s, 2H), 4.06 (s, 3H), 3.46 (s, 3H), 2.63 (s, 3H). ^{13}C NMR (101 MHz, Methanol-d_4) δ 166.56, 163.04, 158.33, 153.41, 152.56, 147.46, 142.86, 133.94, 133.43, 121.64, 121.54, 119.95, 119.81, 114.53, 113.54, 96.08, 66.48, 37.41, 36.21, 8.28. HRMS (AP-ESI) *m/z* calcd for $C_{22}H_{24}N_7O_3$ $[M+H]^+$ 434.1941, found 434.1922.

4-(4-((4-((2,3-Dimethyl-2*H*-indazol-6-yl)(methyl)amino)pyrimidin-2-yl)amino)ph-eno-xy)-*N*-hydroxybutanamide (**9b**). White solid. 55% yield.^{1}H NMR (400 MHz, DMSO-d_6) δ 10.40 (s, 1H), 8.99 (s, 1H), 8.69 (s, 1H), 7.80 (d, *J* = 6.0 Hz, 1H), 7.75 (d, *J* = 8.7 Hz, 1H), 7.59 (d, *J* = 8.9 Hz, 2H), 7.43 (d, *J* = 1.8 Hz, 1H), 6.87 (dd, *J* = 8.8, 1.8 Hz, 1H), 6.79 – 6.74 (m, 2H), 5.75 (d, *J* = 6.0 Hz, 1H), 4.06 (s, 3H), 3.89 (t, *J* = 6.3 Hz, 2H), 3.45 (s, 3H), 2.63 (s, 3H), 2.12 (t, *J* = 7.4 Hz, 2H), 1.91 (p, *J* = 6.7 Hz, 2H). ^{13}C NMR (101 MHz, DMSO-d_6) δ 169.17, 162.88, 159.52, 155.41, 153.55, 147.45, 142.41, 134.56, 132.61, 122.15, 120.86, 120.20, 119.94, 114.73, 114.39, 96.35, 67.44, 38.33, 37.84, 29.27, 25.42, 9.88. HRMS (AP-ESI) *m/z* calcd for $C_{24}H_{28}N_7O_3$ $[M+H]^+$ 462.2254, found 462.2276.

5-(4-((4-((2,3-Dimethyl-2*H*-indazol-6-yl)(methyl)amino)pyrimidin-2-yl)amino)ph-eno-xy)-*N*-hydroxypentanamide (**9c**). White solid. 50% yield.^{1}H NMR (400 MHz, DMSO-d_6) δ 10.37 (s, 1H), 9.11 (s, 1H), 8.67 (s, 1H), 7.79 (d, *J* = 6.2 Hz, 1H), 7.76 (d, *J* = 8.8 Hz, 1H), 7.60 – 7.55 (m, 2H), 7.44 (d, *J* = 1.7 Hz, 1H), 6.88 (dd, *J* = 8.8, 1.8 Hz, 1H), 6.81 – 6.75 (m, 2H), 5.76 (d, *J* = 6.1 Hz, 1H), 4.06 (s, 3H), 3.90 (t, *J* = 5.9 Hz, 2H), 3.46 (s, 3H), 2.63 (s, 3H), 2.01 (t, *J* = 6.7 Hz, 2H), 1.71 – 1.59 (m, 4H). ^{13}C NMR (101 MHz, DMSO-d_6) δ 169.42, 162.85, 158.81, 154.27, 153.90, 147.41, 142.21, 134.03, 132.65, 122.23, 121.16, 120.08,

120.00, 114.73, 114.42, 96.42, 67.66, 38.45, 37.85, 32.41, 28.76, 22.30, 9.88.HRMS (AP-ESI) *m/z* calcd for $C_{25}H_{30}N_7O_3$ $[M+H]^+$ 476.2410, found 476.2489.

6-(4-((4-((2,3-Dimethyl-2*H*-indazol-6-yl)(methyl)amino)pyrimidin-2-yl)amino)ph-eno-xy)-*N*-hydroxyhexanamide (**9d**). White solid. 47% yield. ^{1}H NMR (400 MHz, DMSO-d_6) δ 10.35 (s, 1H), 8.93 (s, 1H), 8.67 (s, 1H), 7.80 (d, *J* = 6.0 Hz, 1H), 7.75 (dd, *J* = 8.7, 0.8 Hz, 1H), 7.60 (d, *J* = 9.1 Hz, 2H), 7.42 (dd, *J* = 1.8, 0.8 Hz, 1H), 6.87 (dd, *J* = 8.8, 1.8 Hz, 1H), 6.75 (d, *J* = 9.1 Hz, 2H), 5.73 (d, *J* = 5.9 Hz, 1H), 4.06 (s, 3H), 3.87 (t, *J* = 6.4 Hz, 2H), 3.45 (s, 3H), 2.63 (s, 3H), 1.97 (t, *J* = 7.3 Hz, 2H), 1.68 (p, *J* = 6.6 Hz, 2H), 1.55 (p, *J* = 7.4 Hz, 2H), 1.43 – 1.33 (m, 2H).HRMS (AP-ESI) *m/z* calcd for $C_{26}H_{32}N_7O_3$ $[M+H]^+$ 490.2567, found 490.2517.

7-(4-((4-((2,3-Dimethyl-2*H*-indazol-6-yl)(methyl)amino)pyrimidin-2-yl)amino)ph-eno-xy)-*N*-hydroxyheptanamide (**9e**). White solid. 53% yield. ^{1}H NMR (400 MHz, DMSO-d_6) δ 10.33 (s, 1H), 8.93 (s, 1H), 8.65 (s, 1H), 7.80 (d, *J* = 6.0 Hz, 1H), 7.75 (d, *J* = 8.7 Hz, 1H), 7.60 (d, *J* = 9.0 Hz, 2H), 7.44 – 7.41 (m, 1H), 6.87 (dd, *J* = 8.8, 1.7 Hz, 1H), 6.75 (d, *J* = 9.0 Hz, 2H), 5.73 (d, *J* = 5.9 Hz, 1H), 4.06 (s, 3H), 3.88 (t, *J* = 6.5 Hz, 2H), 3.45 (s, 3H), 2.63 (s, 3H), 1.99 – 1.91 (m, 2H), 1.67 (dt, *J* = 14.8, 6.8 Hz, 2H), 1.51 (dt, *J* = 14.8, 6.6 Hz, 2H), 1.39 (m, 2H), 1.34 – 1.27 (m, 2H). HRMS (AP-ESI) *m/z* calcd for $C_{27}H_{34}N_7O_3$ $[M+H]^+$ 504.2723, found 504.2746.

4-((4-((2,3-Dimethyl-2*H*-indazol-6-yl)(methyl)amino)pyrimidin-2-yl)amino)benzohy-drazide (**11**).To a solution of **10** (0.40 g, 1.03 mmol) in dichloromethane (10 mL) in ice bath, was added 2-(1H-benzotriazole-1-yl)-1,1,3,3-tetramethyluronium tetrafluoroborate (TBTU, 0.40 g, 1.24 mmol), followed by Et_3N (0.13 g,1.24 mmol). 30 min later, hydrazine hydrate (0.06 g, 1.24 mmol) was added. 12 h later, the solution was diluted by water and extracted with dichloromethane. The combined organic extract was washed with saturated $NaHCO_3$ and brine, dried over Na_2SO_4 overnight, and the solvent was evaporated under vacuum. The crude product was purified by silica gelcolumn chromatography (MeOH/CH_2Cl_2, 1/50 to 1/20) to affordcompound**11**, white solid (0.22 g, 52% yield). ESI-MS *m/z*: 403.21 $[M+H]^+$.

4-((4-((2,3-Dimethyl-2*H*-indazol-6-yl)(methyl)amino)pyrimidin-2-yl)amino)-*N*-prop-ylbenzohydrazide (**12**). Compound **11** (0.60 g, 1.49 mmol) and propionaldehyde (0.10 g, 1.79 mmol) were added to 15 mL anhydrous methanol, then *p*-toluenesulfonic acid (0.025 g, 0.15 mmol) was added at room temperature. 8h later, the reaction solution was filtered and concentrated. The obtained residue was dissolved in 15 mL anhydrous methanol, and $NaBH_3CN$ (0.14 g, 2.24mmol) was added. The pH value of the solution was adjusted to 5 by Conc. HCl/MeOH (v:v=1:1). 12h later, the pH of the solution was adjusted to 8 by saturated $NaHCO_3$. The organic phase was decompressed and evaporated, and the residual was extracted with ethyl acetate. The combined organic extract was washed with saturated $NaHCO_3$ and brine, dried over Na_2SO_4 overnight, and the solvent was evaporated under vacuum. The crude product was purified by silica gel column chromatography (MeOH/CH_2Cl_2, 1/100 to 1/45) to afford compound **12**, white solid (0.21 g, 31% yield). ^{1}H NMR (400 MHz, DMSO-d_6) δ 9.81 (s, 1H), 9.47 (s, 1H), 7.90 (d, *J* =

6.0 Hz, 1H), 7.82 (d, *J* = 8.5 Hz, 2H), 7.77 (d, *J* = 8.8 Hz, 1H), 7.68 (d, *J* = 8.5 Hz, 2H), 7.47 (d, *J* = 1.7 Hz, 1H), 6.90 (dd, *J* = 8.8, 1.7 Hz, 1H), 5.86 (d, *J* = 6.0 Hz, 1H), 5.10 (s, 1H) 4.07 (s, 3H), 3.50 (s, 3H), 2.74 (t, *J* = 7.1 Hz, 2H), 2.64 (s, 3H), 1.47 (q, *J* = 7.3 Hz, 2H), 0.92 (t, *J* = 7.4 Hz, 3H).^{13}C NMR (101 MHz, DMSO-d_6) δ 165.69, 162.90, 159.59, 156.18, 147.48, 144.41, 142.38, 132.62, 128.07, 125.25, 122.20, 120.20, 119.97, 117.84, 114.43, 97.38, 53.72, 38.44, 37.83, 21.32, 12.15, 9.88. HRMS (AP-ESI) *m/z* calcd for $C_{24}H_{29}N_8O_1$ $[M+H]^+$445.2464, found 445.2478.

In vitro HDACs inhibition assay

In vitro HDACs inhibition assays were conducted according to the reported methods [12]. Briefly, 10 μL of enzyme solution (HDAC1, HDAC4, HDAC6 or HDAC11) was mixed with different concentrations of tested compound (50 μL). The mixture was incubated at 37℃ for 5 mins, followed by adding 40 μL fluorogenic substrate (Boc-Lys(acetyl)-AMC for HDAC1 and HDAC6, Boc-Lys(triflouroacetyl)-AMC for HDAC4, Ac-Leu-GlyLys(Ac)-AMC for HDAC11). After incubation at 37℃ for 30 mins, the mixture was quenched by adding100 μL of developer containing Trichostatin A (TSA) and trypsin. After another 20 min of incubation at 37 ℃, fluorescence intensity was measured using a microplate reader at excitation and emission wavelengths of 390 and 460 nm, respectively. The inhibition ratios were calculated from the fluorescence intensity readings of tested wells relative to those of control wells, and the IC_{50} values were calculated using nonlinear regression with normalized dose-response fit using Prism GraphPad software.

In vitro VEGFRs inhibition assay

VEGFR1, VEGFR2 and VEGFR3 inhibitory activity was measured using Kinase-Glo^{TM} Luminescent Kinase Assay by HUAWEI PHARMA (Ji'nan, China). In brief, the tested compounds, kinases, substrate, and ATP were diluted in kinase buffer to the indicated concentrations, covered the assay plate, and incubated at room temperature for 40 min, then the Kinase-Glo reagent was added. Over an additional 15 min of incubation, the luminescence was recorded on a microplate reader (SpectraMax M5). The IC_{50}values were calculated using nonlinear regression with normalized dose-response fit using Prism GraphPad software.

In vitro anti-proliferative assay

All cell lines were maintained in RPMI1640 medium containing 10% FBS at 37℃ in a 5% CO_2 humidified incubator. Antiproliferation assay was determined by the MTT (3-[4,5-dimethyl-2-thiazolyl]-2,5-diphenyl-2h-tetrazoliumbromide) method. Briefly, cells were passaged the day before seeded into a 96-well plate, allowed to grow for 12 h, and then treated with different concentrations of compound for 48 h. A 0.5% MTT solution was added to each well. After incubation for another 4 h, formazan formed from MTT was extracted by adding 200 uL of DMSO. Absorbance was then determined using an ELISA reader at 570 nm.

HUVECs tube formation assay

HUVEC tuber formation assay was conducted according to the reported methods [12]. Briefly, matrigel (100 μL; BD biosciences, NJ) was added into test well of 96-well plates and then allowed to polymerize

for 0.5 h at 37 °C. HUVECs were trypsinized and seeded at the density of 40000 per well in M199 (5% FBS) containing DMSO or test compounds for 6 h at 37 °C in a CO_2 incubator. The morphological changes of the cells and tubes formation were observed under a phase-contrast microscope (OLYMPUS IX51) and photographed at a 200 magnification. Experiments were repeated at least two times.

Rat thoracic aorta ring (TARs) assay

TARs assay was conducted according to the reported methods [12]. Briefly, matrigel (100 μL; BD biosciences, NJ) was added into test well of 96-well plates and then allowed to polymerize for 0.5 h at 37 °C. Sprague–Dawley rats of 4 to 6-week-old were sacrificed and aortas were harvested. Each aorta was cut into 1-mm slices and embedded in additional 100 μL of matrigel in 96-well plates. After that, the rings were incubated for 30 min at 37 °C and 5% CO_2. Aorta rings were treated with vehicle or tested compounds each day for 6 days and photographed on the 7th day at ×200 magnification. Experiments were repeated at least two times.

Western blot analysis

A549 or HUVEC cells were treated with compounds or DMSO for a specified period of time. Then the cells were washed twice with cold PBS and lysed in ice-cold RIPA buffer. Lysates were cleared by centrifugation. Protein concentrations were determined using the BCA assay. Equal amounts of cell extracts were then resolved by SDS-PAGE, transferred to nitrocellulose membranes and probed with ac-histone H4 antibody, ac-α-tubulin antibody, β-actin antibody, phosphorylated VEGFR2 antibody and total VEGFR-2 antibody, respectively. Blots were imaged using an enhanced chemiluminescence system.

In vitro liver microsomal stability assay

Mice liver microsomes containing tested compounds were incubated with NADPH at 37 °C. At the specific time points, acetonitrile was added to the samples to terminate the reaction, then the samples were subjected to vortex mixing for 5 min and stored in a freezer at -80 °C. Before analysis, the samples were centrifuged at 4000 rpm for 15 min. The remaining of tested compounds in the supernatants were analyzed by LC-MS/MS. The $t_{1/2}$ values were calculated using the equation $t_{1/2} = -0.693/k$, where k is the slope found in the linear fit of the natural logarithm of the fraction remaining of tested compounds vs. incubation time.

Results And Discussion

Compound Design and Synthesis

Compounds **5**, **7**, **9a-9e** were designed by replacing the amide connecting unit of **ZYJ-13f** with reverse amide, secondary amine, and ether, respectively (**Figure 2**). Besides, the N-acyl *o*-diaminobenzene zinc binding group of **JMC-6d** was changed to hydrazide due to the good metabolic stability of hydrazide [13], leading to compound **12**(**Figure 2**).

Scheme 1. Synthesis of Compounds 5,7 and 9a–9e

Reagents and conditions: (a) benzene-1,4-diamineor 4-aminophenol, isopropanol, conc HCl, reflux, 4 h; (b) suberic acid monomethyl ester, TBTU, TEA, anhydrous DMF, ice bath, 30 min, rt, 12 h; (c) $NH_2OH.HCl$, KOH, anhydrous CH_3OH, rt, 2 h; (d) methyl 6-bromohexanoate, K_2CO_3, DMF, reflux; (e) various methyl ω-bromoalkanoates, Cs_2CO_3, DMF, reflux.

The procedures to synthesize the target compounds **5**,**7** and **9a**-**9e** were outlined in Scheme 1. Compound **1**, which was obtained according to the previous methods [12], was treated with 4-aminophenolandbenzene-1,4-diamine to produce the key intermediates **2** and **3**, respectively. The intermediate **3** reacted with suberic acid monomethyl ester by TBTU-mediated amide condensation to afford the intermediate **4**, which was transformed to hydroxamic acids **5**. In addition, the intermediate **3** could also react with methyl 6-bromohexanoate by nucleophilic substitution to get compound **6**, which could be transformed to hydroxamic acids **7**. The intermediate **2** reacted with various methyl ω-bromoalkanoates by nucleophilic substitution reaction to get compounds **8a**-**8e**, respectively, which were further converted into target hydroxamic acids **9a**-**9e**.

Scheme 2. Synthesis of Compound **12**

Reagents and conditions: (a) $N_2H_4{\cdot}H_2O$, TBTU, TEA, DCM; (b) 1) propionaldehyde, *p*-toluenesulfonic acid, CH_3OH; 2) $NaBH_3CN$, rt.

The procedures to synthesize the target compound **12** was outlined in Scheme 2. Compound**10**, obtained according to the previous methods [12], reacted with hydrazine hydrate by TBTU-mediated amide formation to afford the intermediate **11**. Then reductive amination of **11** afforded the target hydrazide**12**.

In Vitro HDAC and VEGFR Inhibition Assay

The HDAC and VEGFR inhibitory potency of all target compounds were preliminarily tested by determining the HDAC1, HDAC6 and VEGFR2 inhibition rates at 0.5 μM, respectively. The approved pan-HDAC inhibitor SAHA, the clinical class I selective HDAC inhibitor MS275, and the approved VEGFR inhibitor pazopanib were used as the positive controls. Results in Table 1 revealed that most target compounds could effectively inhibit all three enzymes with inhibition rates over 50% at 0.5 μM. Generally, hydroxamates with linker length over three methylenes (**5**, **7**, **9c**, **9d**, **9e**) were more potent HDAC inhibitors than compounds with shorter linkers (**9a**, **9b**). Note that the hydrazide compound **12** exhibited HDAC1 selective inhibition over HDAC6, which was similar to the positive control MS275.

Table 1. Invitro HDAC and VEGFR inhibitory activities of all target compounds

Compound	Structures	Inhibition rate at 0.5μM[a]		
		HDAC1	HDAC6	VEGFR2
5		95%	94%	100%
7	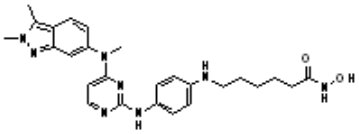	99%	93%	99%
9a	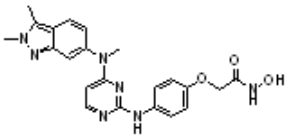	78%	78%	100%
9b	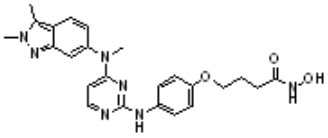	83%	74%	100%
9c	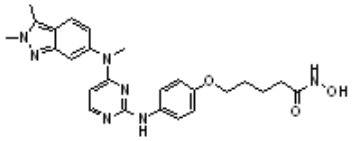	96%	95%	100%
9d	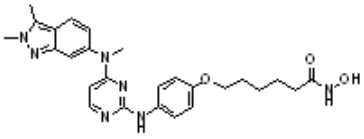	94%	91%	99%
9e	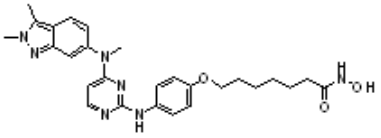	96%	94%	97%
12	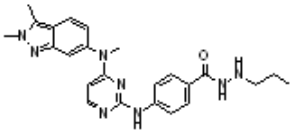	68%	4%	100%
SAHA	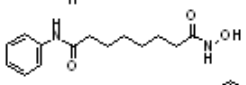	94%	96%	ND[b]
MS275	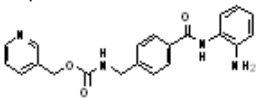	72%	6%	ND[b]
Pazopanib	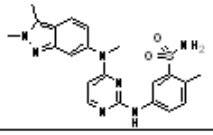	ND[b]	ND[b]	100%

[a]Assays were performed in duplicate; [b]Not determined.

In vitro antiproliferative assay

Considering their promising HDAC inhibitory activities, compounds **5**, **7** and **9c**, **9d**, **9e** and **12** were further tested in antiproliferative assay against five solid tumor cell lines. Results in Table 2 showed that compounds **5**, **9e** and **12** were three most potent compounds with IC_{50} values lower than 5 μM against all tested cancer cell lines. Remarkably, the overall antiproliferative activities of **5**, **9e** and **12** were even more

potent than the two clinical HDAC inhibitors, SAHA and MS275. Consist with the previously reported results [12], VEGFR inhibitor pazopanib possessed negligible cytotoxicity.

Table 2. In vitro antiproliferative activities of selected compounds

Compound	IC_{50} (μM)[a]					
	A549	HCT116	HeLa	A2780	HepG2	MDA-MB-231
5	2.15	2.07	3.14	4.07	3.22	4.85
7	4.52	3.21	4.95	ND[b]	5.94	>10
9c	4.69	5.46	>10	7.54	>10	>10
9d	5.36	6.10	>10	8.12	>10	ND[b]
9e	2.44	2.39	3.52	4.47	2.52	4.13
12	3.78	2.59	3.68	4.82	3.04	4.50
SAHA	4.91	4.69	>10	>10	>10	>10
MS275	3.54	3.06	>10	4.03	>10	>10
Pazopanib	>10	ND[b]	>10	>10	>10	>10

[a] Assays were performed in replicate (n ≥2),the SD value are <20% of the mean. [b]Not determined.

In vitro HUVECs tube formation assay

Compounds **5**, **9e** and **12**were progressed to *in vitro* HUVECs tube formation assay to evaluate their antiangiogenesis activities. The test concentration of compounds was set at 0.5 μM, which is lower than their antiproliferative IC_{50} values to avoid cytotoxicity against HUVECs. It has been demonstrated that **5**, **9e** and **12** could significantly inhibit the HUVECs tube formation, just like the positive control pazopanib (**Figure 3**).

Ex vivo rat thoracic aorta ring (TARs) assay

Ex vivo rat TARs assay was carried out to further validate the antiangiogenic activities of compounds **5**, **9e** and **12**, which clearly showed that compounds **5**, **9e** and **12** could almost completely inhibit the microvessel outgrowth as well as pazopanib (**Figure 4**).

HDAC and VEGFR selectivity profiling

Zn^{2+}-dependent HDAC family contains 11 isoforms, which can be categorized into class I (HDAC 1, 2, 3, and 8), class IIa (HDAC4, 5, 7, and 9), class IIb (HDAC6, and 10) and class IV (HDAC11)[14].To profile the selectivity of our HDAC and VEGFR dual inhibitors, the IC_{50} values of compounds **5**, **9e** and **12** against

HDAC1, HDAC4, HDAC6 and HDAC11were determined with SAHA and MS275 as the positive controls (Table 3).Compared with SAHA, hydroxamates **5** and **9e** showed comparable even slightly better inhibitory activities against HDAC1 and HDAC6, the representative isoforms of class I and class IIb HDAC, respectively. Similar to SAHA, the hydroxamates **5** and **9e** were not potent inhibitors against class IIa isoform HDAC4 and class IV isoform HDAC11. Similar to MS275, the hydrazide **12** exhibited high selectivity of HDAC1 over other tested isoforms, indicating the class I selectivity. Moreover, compounds **5**, **9e** and **12** were tested against VEGFR1, VEGFR2 and VEGFR3 to profile their VEGFR isoform selectivity. As well as pazopanib, compounds **5**, **9e** and **12** exhibited potent pan-VEGFR inhibition with no significant discrimination among VEGFR family members (Table 3).

Table3.HDACs and VEGFR isoform selectivity of selected compounds

Compound	IC_{50} (μM)[a]						
	HDAC1	HDAC4	HDAC6	HDAC11	VEGFR1	VEGFR2	VEGFR3
5	0.12	>10	0.094	>10	0.018	0.016	0.054
9e	0.24	9.17	0.063	>10	0.041	0.032	0.066
SAHA	0.15	>10	0.085	>10	ND[b]	ND[b]	ND[b]
12	0.42	>10	8.96	>10	0.034	0.025	0.037
MS275	0.26	>10	>10	ND[b]	ND[b]	ND[b]	ND[b]
pazopanib	ND[b]	ND[b]	ND[b]	ND[b]	0.034	0.010	0.015

[a] Assays were performed in replicate (n ≥2), the SD value are <20% of the mean. [b] Not determined.

Western blot analysis

Western blot analysis was performed to valid the intracellular target engagement of compounds **5** and **12**. Results in **Figure 5A**showed that both **5** and **12** could remarkably increase the levels of acetyl-histone H4 (Ac-HH4), which is the intracellular substrate of class I HDACs. Besides, compound **5** could also increase the levels of acetyl-α-tubulin(Ac-Tub), the substrate ofHDAC6, while compound **12** showed no effects on Ac-Tub. These results were in line with their HDAC isoform selectivity presented in Table 3. The inhibition of intracellular VEGFR by compound **12** and **5**was confirmed by the decreased levels of phosphorylated VEGFR2 (p-VEGFR2) in HUVECs (**Figure 5B**).

In vitro liver microsomal stability assay

Considering their promising in vitro activities, the metabolic stability in mouse liver microsome of compounds **5**, **9e** and **12** were determined and compared with that of pazopanib. Unfortunately, no compounds possessed superior metabolic stability relative to pazopanib (Table 4).

Table4. Metabolic stability in mouse liver microsome of selected compounds

Compound	**5**	**9e**	**12**	**pazopanib**
$t_{1/2}$(min)[a]	4.1	9.2	7.8	15.2

[a] Assays were performed in duplicate.

Conclusion

A novel series pazopanib analogs were developed as HDAC and VEGFR dual inhibitors. Compared with pazopanib, many HDAC and VEGFR dual inhibitors exhibited superior cytotoxicity against multiple solid tumor cell lines, which could be ascribed to their potent HDAC inhibition. Moreover, compounds **5**, **9e** and **12** also exhibited uncompromised VEGFR inhibitory activities and uncompromised antiangiogenic capacities relative to pazopanib. Following work should be focused on structural optimization of these analogs to improve their pharmacokinetic properties, which will lead to multitarget compounds within vivo antitumor activity.

Declarations

Ethics approval and consent to participate

This article does not contain any studies with human participants or animals performed by any of the authors.

Consent for publication

Not applicable.

Availability of data and materials

All data generated or analysed during this study are included in this published article.

Competing interests

The authors declare that they have no competing interests.

Funding

This study was funded by grants from the National Natural Science Foundation of China (Grant No. 82073872).

Authors' contributions

XX and ZXG designed the project. LLN and LY performed the enzymatic screening; LYX, ZYJ and ZJ synthesized the molecules; WYJ, SDQ and LY, JW performed the in vitro experiments. XX analyzed the data and wrote the manuscript.

Acknowledgements

Not applicable.

Authors' information (optional)

Xia Xue

Department of Pharmacy, The Second Hospital, Cheeloo College of Medicine, Shandong University, Jinan, Shandong 250012, PR China; Key Laboratory of Chest Cancer, Shandong University, Jinan, Shandong , PR China.

Yingjie Zhang

Department of Medicinal Chemistry, School of Pharmaceutical of Science,Shandong University , Ji'nan , Shandong 250012 , PR China.

Yongxiang Liao

Advanced Medical Research Institute, Cheeloo College of Medicine, Shandong University, Jinan, Shandong 250012, PR China.

Deqing Sun, Lina Li, Ying Liu, Yongjie Wang

Department of Pharmacy, The Second Hospital, Cheeloo College of Medicine, Shandong University, Jinan, Shandong 250012, PR China.

Wen Jiang, Jian Zhang Yun Luan

Institute of Medical Science, Central Research Laboratory, The Second Hospital, Cheeloo College of Medicine, Shandong University, Jinan, Shandong 250012, PR China.

Xiaogang Zhao

Department of Thoracic Surgery, The Second Hospital, Cheeloo College of Medicine, Shandong University, Jinan, Shandong 250012, PR China; Key Laboratory of Chest Cancer, Shandong University, Jinan, China.

Compliance with Ethical Standards

Disclosure of potential conflicts of interest

All authors declare that they have no conflict of interest.

Research involving Human Participants and/or Animals

Not applicable.

Informed consent

For this type of study, informed consent is not required.

References

1. Susan E, Bates (2020) Epigenetic Therapies for Cancer. N Engl J Med 383:650–663
2. Zagni C, Floresta G, Monciino G, Rescifina A (2017) The search for potent, small-molecule HDACIs in cancer treatment: a decade after Vorinostat. Med Res Rev 37:1373–1428
3. Ali I, Conrad RJ, Verdin E, Ott M (2018) Lysine Acetylation Goes Global: From Epigenetics to Metabolism and Therapeutics. Chem Rev 118:1216–1252
4. Wu P, Nielsen TE, Clausen MH (2015) FDA-approved small-molecule kinase inhibitors. Trends Pharmacol Sci 36:422–439
5. Musumeci F, Radi M, Brullo C, Schenone S (2012) Vascular endothelial growth factor (VEGF) receptors: drugs and new inhibitors. J Med Chem 55:10797–10822
6. Choueiri TK, Escudier B, Powles T, Mainwaring PN, Rini BI, Donskov F, Hammers H, Hutson TE, Lee JL, Peltola K, Roth BJ, Bjarnason GA, Géczi L, Keam B, Maroto P, Heng DY,Schmidinger M, Kantoff PW, Borgman-Hagey A, Hessel C, Scheffold C, Schwab GM, Tannir NM, Motzer RJ,METEOR Investigators(2015) Cabozantinib versus Everolimus in Advanced Renal-Cell Carcinoma. N Engl J Med 373:1814–1823
7. Vyse S, McCarthy F, Broncel M, Paul A, Wong JP, Bhamra A, Huang PH (2018) Quantitative phosphoproteomic analysis of acquired cancer drug resistance to pazopanib and dasatinib. J Proteomics 170:130–140
8. Chan D, Zheng Y, Tyner JW, Chng WJ, Chien WW, Gery S, Leong G, Braunstein GD, Koeffler HP (2013) Belinostat and panobinostat (HDACI): in vitro and in vivo studies in thyroid cancer. J Cancer Res Clin Oncol 139:1507–1514
9. Booth L, Roberts JL, Sander C, Lee J, Kirkwood JM, Poklepovic A, Dent P (2017) The HDAC inhibitor AR42 interacts with pazopanib to kill trametinib/dabrafenib-resistant melanoma cells in vitro and in vivo. Oncotarget 8:16367–16386
10. Tavallai S, Hamed HA, Grant S, Poklepovic A, Dent P (2014) Pazopanib and HDAC inhibitors interact to kill sarcoma cells. Cancer Biol Ther 15:578–585
11. Aggarwal R, Thomas S, Pawlowska N, Bartelink I, Grabowsky J, Jahan T, Cripps A, Harb A, Leng J, Reinert A, Mastroserio I, Truong TG, Ryan CJ, Munster PN (2017) Inhibiting Histone Deacetylase as a Means to Reverse Resistance to Angiogenesis Inhibitors: Phase I Study of Abexinostat Plus Pazopanib in Advanced Solid Tumor Malignancies. J Clin Oncol 35(11):1231–1239. doi:10.1200/JCO.2016.70.5350
12. Zang J, Liang X, Huang Y, Jia Y, Li X, Xu W, Chou CJ, Zhang Y (2018) Discovery of Novel Pazopanib-Based HDAC and VEGFR Dual Inhibitors Targeting Cancer Epigenetics and Angiogenesis Simultaneously. J Med Chem 61:5304–5322

13. McClure JJ, Zhang C, Inks ES, Peterson YK, Li J, Chou CJ (2016) Development of Allosteric Hydrazide-Containing Class I Histone Deacetylase Inhibitors for Use in Acute Myeloid Leukemia. J Med Chem 59:9942–9959
14. Yoshida M, Kudo N, Kosono S, Ito A (2017) Chemical and structural biology of protein lysine deacetylases. Proc Jpn Acad Ser B Phys Biol Sci 93:297–321

Figures

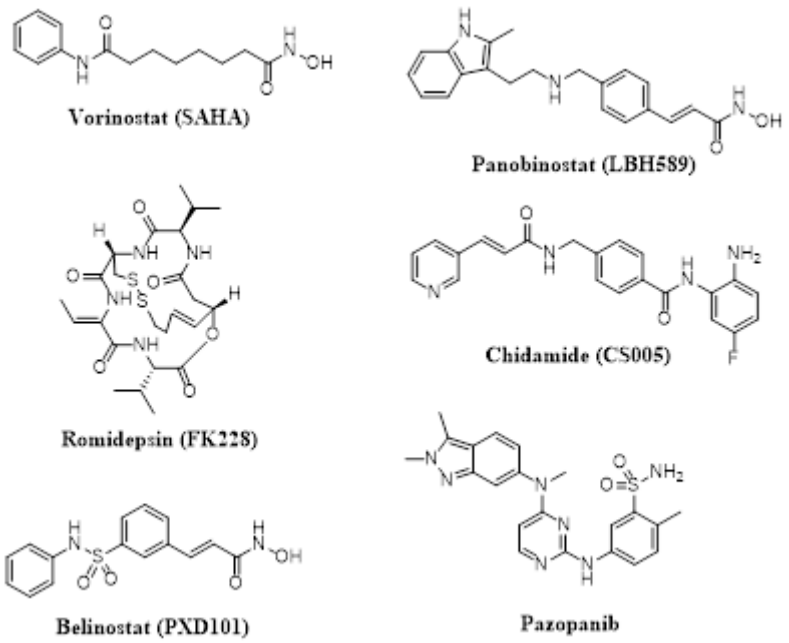

Figure 1

The structures of five approved HDAC inhibitors (vorinostat, romidepsin, belinostat, panobinostat, chidamide) and one approved VEGFR inhibitor pazopanib.

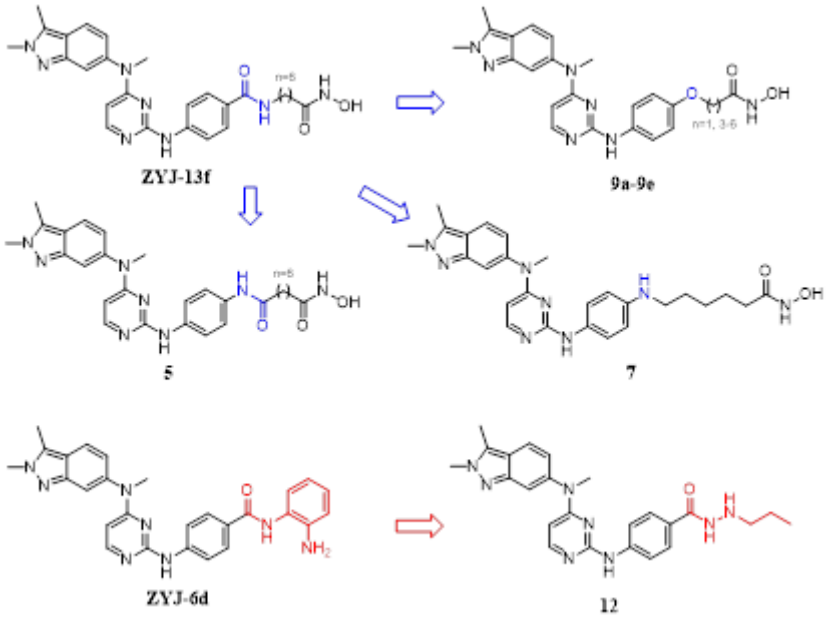

Figure 2

The design strategy and chemical structures of novel HDAC and VEGFR dual inhibitors derived from JMC-13f and JMC-6d.

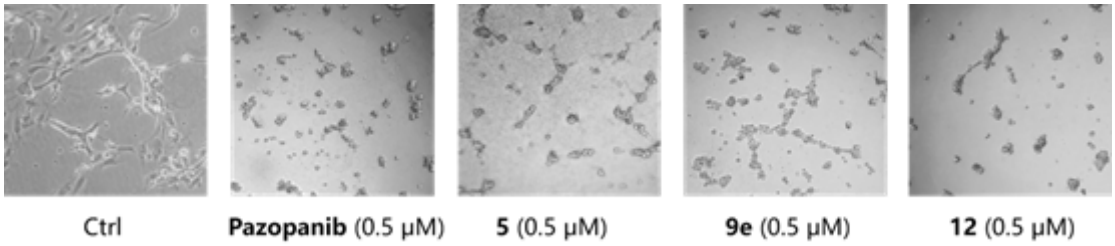

Figure 3

Representative images of the tubular network of HUVECs treated with DMSO or compounds.

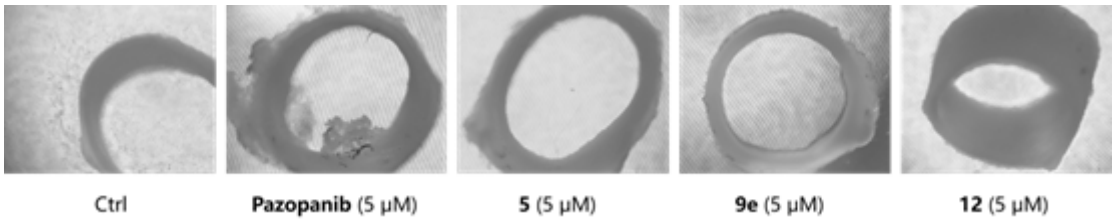

Figure 4

Representative images of rat TARs treated with DMSO or compounds.

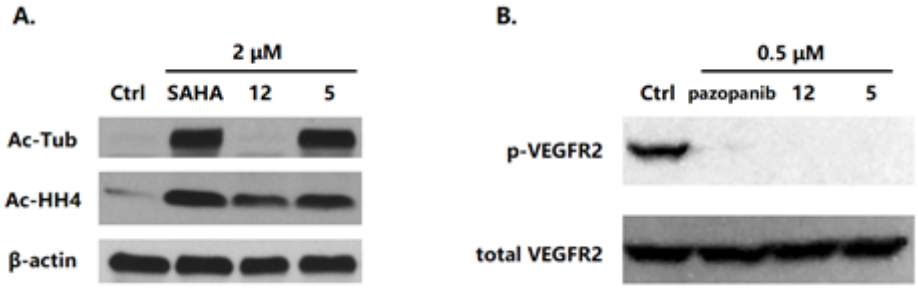

Figure 5

A.A549 cells were treated with DMSO or compounds(2 μM) for 5 h. The levels of indicated proteins were determined by immunoblotting. β-Actin was used as a loading control. B. HUVECs were treated with DMSO or compounds (0.5 μM) for 2 h, then stimulated with VEGF (50 ng/ml). The levels of p-VEGFR2 were determined by immunoblotting. β-Actin and total VEGFR-2 were used as loading controls, respectively.

Supplementary Files

This is a list of supplementary files associated with this preprint. Click to download.

- Scheme01.png
- Scheme02.png